Kinematics Simulation Based on Fluent of a Bionic Manta ray Robot

1st Pengxiao Bao
Beijing Instituite of technology
School of Life Science
Beijing, China
3220201341@bit.edu.cn

2nd Liwei Shi*
Beijing Instituite of technology
School of Life Science
Beijing, China
shiliwei@bit.edu.cn

3rd Zhongyin Zhang
Beijing Instituite of technology
School of Life Science
Beijing, China
zhangzhongyin@bit.edu.cn

4th Shuxiang Guo**
Beijing Instituite of technology
School of Life Science
Beijing, China
guoshuxiang@bit.edu.cn

***Abstract*—The underwater robots are becoming a new direction of robotics in the future because of the increasingly demand on exploring the ocean. Due to thousands of years of evolution, marine organisms have better adaptance to the ocean. In order to design a more reasonable underwater robot, we analyzed different driving mode fishes as the bionic prototype and after comparision, we choose manta ray as our bionic object. A three-dimensional kinematic equation of in-situ flapping wing under body coordinate system is given. And Solidworks is used to simplify and imitate the appearance of the manta fish. As well, we use ANSYS Fluent to simulate the dynamic pressure and velocity magnitude during the period of flapping fins and observe the formation and shedding of high-pressure center and high-velocity center, which is consistent with actual manta fish. Also we discuss the relationship between pressure, frequency and amplitude. The whole experiments proved that the manta fish prototype has great potential as a underwater propeller.**

Keywords—Computational Fluid Dynamics(CFD), bionics, underwater vechicles, bionics, manta

I. Introduction

In order to adapt to the changing environment, the organisms on the earth have formed their own unique morphological structure and life system in the long process of evolution. The imitation of these characteristics is the prototype of bionics in the field of aesthetic architecture [1], structure bionics [2-4], new material [5-6], swarm intelligence algorithm [7-9], biosensor [10-11], mechanical bionics, motion bionics and so on. So far, Bionics productions have played an essential role in aerospace, visual imaging, new materials, robotics, architectural design, algorithm, pharmacy and other fields.

Recently, underwater robot has become an important tool to explore the ocean, whose strategic position is increasingly prominent. Underwater robots have important applications in underwater search and rescue, marine archaeology, seabed exploration, fishery, ship maintenance and so on. Because the seabed topography, ocean current and many other factors cause the complexity of the marine environment [12], it will increase the difficulty of designing an underwater unmanned vehicle. Due to the evolution of marine organisms for millions of years, its biological structure has strong adaptability to the marine environment. It's easier for an bionic underwater robot based on marine life to complete specific functions with lower cost and is more friendly to the marine ecosystem.

The movement modes of aquatic organisms can mainly be divided into three categories. Body and / or caudal fin propulsion(BCF), median and/or paired fin propulsion(MPF), jet propulsion(JET). The design of Underwater Bionic Robot also refers to these typical motion modes. The prototype of underwater bionic robot includes turtle, tortoise, jellyfish, squid, eel fish, manta ray, snake, tunas and so on.

Robobee, a bionic bee robot developed by Harvard University, can fly across water-air media [13]. T.Wang developed a bionic dredging turtle to clean underwater silt in artificially constructed rivers [14]. Y.Wang design a bionic scallop robot based on jet propulsion that can move up to 1.8 body length per second and has many potential applications for its good swimming continuity, stable swimming, strong protection, and low-cost structure [15]. Y.Chen propose a soft robotic eel and flexibly perform linear motion and turning motion [16]. L. Li explore the energy cost of the follower when swimming close to a neighbour in 3D formations with robotic fish [17]. Q. Zhao introduce a micro-robotic fish that is highly efficient compared with conventional motors and piston-based robotic fish [18] .

Therefore, we designed a prototype based on the manta ray, and carried out kinematics simulation experiments with ANSYS fluent. This paper presents a flapping-mode motion function and gives a three-dimensional kinematic equation of in-situ flapping wing under body coordinate system. The flapping mode of the manta ray is simulated and results show that the high-pressure center and high-velocity center movement is consistence with the actual condition. At last, we discuss the relationship between frequency, propulsion pressure and amplitude. The fish flapping-wing swimming mode is convinced to be a good propeller and the underwater robot designation based on manta ray is feasible.

II. Biological Inspiration and Modeling

A. Bionic Prototype Research

BCF mode is the most common mode of fish locomotion, contracting mainly the whole-body muscles to cause the body to undergo undulation waves and thus generate the driving force. BCF model can be divided into ostraciidae mode, eel model, carangidae model, sub-carangidae model and blenniidae model.

MPF fish are mainly propelled by fins other than caudal fin, such as pectoral fin, dorsal fin and ventral fin. According to the specific way of fin movement, it can be divided into two modes,one is the flapping wing mode and the other is the wave mode. MPFs can be divided into three groups according to the site of the fin, one being the family of rajidae, diodontidae, labridae that utilize the pectoral fin as their main motor propulsion; gymnotidae families that adopt a ventral fin for propulsion; tetraodontidae and balistidae, which adopt a common advance with a dorsal and ventral fin.

JET is commonly found in jellyfish and cuttlefish, and this motion way is mainly performed by suction and drainage through a pump-like device, driving the underwater robot forward through a recoil force generated by prompt drainage,

National Natural Science Foundation of China (61773064, 61503028)

978-0-7381-4657-7/21/$31.00 ©2021 IEEE

and this motion way of Underwater Bionic Robot is well oriented, convenient to make, and high acceleration[19].

MPF swimming mode integrates high propulsion efficiency, excellent mobility and stability, which is not only suitable for ocean navigation, but also has the characteristics of low-speed flexible mobility and strong anti-disturbance ability, which is suitable for offshore and other complex environments. Otherwise, the swimming process only depends on the wave propulsion of pectoral fins and the other parts are very similar to a rigid body. The rigid part can be designed into a large internal space to accommodate various scientific detection instruments.Therefore, we choose the manta fish as the bionic prototype.

B. Kinematic Analysis of Manta fish

According to the MPF mode, the fin motion mode can be divided into two modes, one is the flapping wing mode and the other is the wave mode. Either way, when the manta fish moves, traveling waves will travel from head to tail in the direction of body length and the waves are presented on symmetrical pectoral fins on both sides .

Fig. 1. Coordinate system of the manta fish motion

A point on the middle line of the fish was chosen as the base point. The direction of the tail-head connection is *y* and the spread direction of pectoral fin is *x*. According to the right-hand rule, we can get the z-axis. The coordinate system is shown in fig.1 ,which is set up to describe the motion of the manta fish. The swimming period of the manta fish can be regarded as a traveling wave. Therefore, set up formula(1) to describe the traveling waves.

$$z(t) = s\ (t)\ A(x)\sin(2\pi ft - \frac{2\pi y}{\lambda} + \phi) \tag{1}$$

f represents the frequency of waves. λ represents the wavelength. ϕ represents the phase difference between tangential propagation and spread propagation. x represent the coordinates of a pectoral fin point on direction x and y represent the coordinates of a pectoral fin point on direction y.

In this formula, *s(t)* is the starting period function, and ST represent the start-up period of time and the function only works in the transition state of the manta fish.

$$s(t) = \begin{cases} 0 & t = 0 \\ \frac{1}{ST}t - \frac{1}{2\pi}\sin(\frac{2\pi}{ST}) & 0 < t < ST \\ 1 & t = 1 \end{cases} \tag{2}$$

$A(x)$ is amplitude control function. And it depends on the type of manta fish.

$$A(x) = (c_0 + c_1 x + c_2 x^2) \tag{3}$$

c_0 , c_1 , c_2 is the pectoral fin envelop ratio. When $c_1 = c_2 = 0$, it represents a constant traveling wave is propagating in a tangential direction. When $c_0 = c_2 = 0$, it describes a combination of a constant tangential propagation and a linear increase in the oscillation of the spread direction. When $c_2 \neq 0$, the equation describes the combination of the traveling wave of tangential direction and the oscillation of the spread direction whose amplitude increases linearly.

Suppose the manta fish is at a constant condition and no phase difference between tangential propagation and spread propagation. At this time, the starting period function $s(t)$ doesn't work. Due to the current time position coordinates are related to the previous time position and speed. We can get the kinematics equation(4-6) of the manta fish under the set coordinate system.

$$x^{t+1} = x^t + v_x \times dt \tag{4}$$

$$y^{t+1} = y^t + v_y \times dt \tag{5}$$

$$z^{t+1} = z^t - 2\pi f \times A(x)\cos(\frac{2\pi y}{\lambda} - 2\pi ft) \tag{6}$$

According to observation, the movement of manta ray can be divided into rigid motion and flexible motion [20]. The fish body and tail of ray are translation motion, while the fin of ray is flexible deformation movement. In this paper, we ignore the forward velocity and only discussed the oscillating of the manta fish.

C. Shape Simplification and Modeling

The pectoral fin shape of manta fish is irregular oval or triangle[21-24]. The size of the oval body is about 50-100cm in general, while the size of triangle manta fish can reach about 1.44m in general, and some kinds can reach a width of 8m. Among all, the body shape of the manta fish is flat and the wing span is longer than the body length. We set the wing span *C* as 2m and the body length *L* as 1.29m.

As the motion of the manta ray is mainly devoted by the movement of pectoral fins, the head fin, dorsal fin, eye, nose, mouth, gill and so on are simplified.

We use SolidWorks to modeling the manta fish and the appearance of the manta fish is as shown in Fig.2. Because the pectoral fins are symmetrical, we only give the function of the right pectoral fin. And the upwind surface function of the pectoral fin is as formula(9).

$$y = \begin{cases} -0.01x^2 - 0.03x + 42.27 & 0 < x \le 15 \\ 0.0015x^2 - 0.36x + 44.8 & 15 < x \le 30 \\ 0.0015x^2 - 0.423x + 47 & 30 < x \le 46 \\ 0.0015x^2 - 0.577x + 54 & 46 < x \le 65 \\ 0.0015x^2 - 0.75x + 65.4 & 65 < x \le 85 \\ -0.01x^2 + 1.14x + 11.84 & 85 < x \le 100 \end{cases} \tag{9}$$

And the downwind surface function of the pectrol fin is as formula(10).

$$y=\begin{cases}16x-86.75 & 0<x\le 4\\ 0.00055x^3-0.06x^2+2.2x+30.6 & 4<x\le 30\\ -0.001x^3+0.104x^2-3.572x+40 & 30<x\le 45\\ 0.0015x^2-0.174z-0.454 & 45<x\le 85\\ 0.0095x^2-1.4725x+47 & 85<x\le 100\end{cases} \quad (10)$$

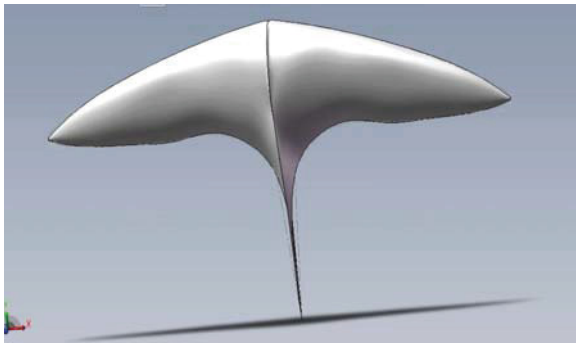

Fig. 2. Model of the manta fish by Solidworks

III. Simulation and Analysis

The kinematics simulation is based on ANSYS Fluent, which is a finite element software package that can be used to solve the problems of structure, fluid, electric power, electromagnetic field and collision.

The software mainly includes three parts: pre-processing module, analysis and calculation module and post-processing module. In this paper, pre-processing progress is processed by ICEM-CFD and post-processing progress is processed by CFD-POST.

A. Mesh set up

The fish model was imported into ICEM CFD. The calculation region is first established and we define global parameters, including global grid size, layer height, grid type and grid generation method. The grid density should be higher in the place where the gradient of flow field is larger, and it can be lower in the place where the gradient of flow field is smaller. Therefore, the mesh density should be higher when it is close to the manta fish.

We create a cylindrical calculation domain . Part inlet is a circle with a radius of 1.5m. And the length of the calculation is 4m and is three times more than the body length and we suppose that the flow field can be fully developed in this case.

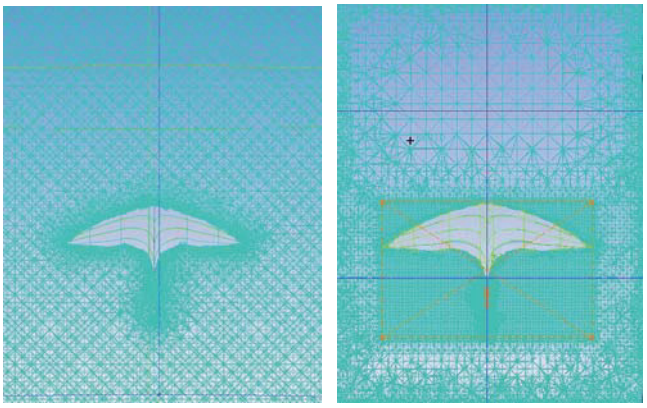

(a)mesh cut plane before encryption (b)mesh cut plane after encryption

Fig. 3. Mesh cut planes

When setting up the mesh, we use the tetra/mixed type to generate tetrahedral mesh. And use the Robust method to calculate the mesh. The global size is set as 40, the surface of part mesh is 6, the height is 4, the number of layers is 12. The type of the surface mesh is all tri and the surface calculation method is Independent Patch. In order to improve the accuracy, we densify the mesh around the fish and particularly create the mesh density around the manta fish tail. Total cells are 1852364. Figure 3 is the mesh cut plane before and after encryption.

B. Static Simulation

Import the mesh into fluent and check the mesh volume. If there is negative volume mesh, the calculation will be interrupted.

Define the flow velocity of the inlet to be 0.1m/s. Observe the pressure on the surface of the manta fish.

$$u(x,y,z)|_{t=0}=0.1 \quad (11)$$

The surface of manta fish is a wall model. There is no fluid passing through the fish body and the fish body is always in contact with the fluid.

$$u(x,y,z)|^{n}_{\Gamma(t)}=0.1 \quad (12)$$

$$u(x,y,z)|_{\Gamma}=u_{\Gamma} \quad (13)$$

$\Gamma(t)$ represent the contact surface of the fish body and the fluid. And the velocity of the fluid and the velocity of the fish are always equal on the boundary of the contact surface. The inlet is the velocity-boundary inlet and the outlet is the pressure-based outlet. Therefore, we can obtain formula(14).

$$\frac{\partial(p,u)}{\partial n}=0 \quad (14)$$

The static pressure of fish body under hydro static flow is shown in the fig.4. It can be derived that in still water, the resultant force received by the fish body is approximately zero in direction z and direction x, and the velocity in direction y is approximately zero.

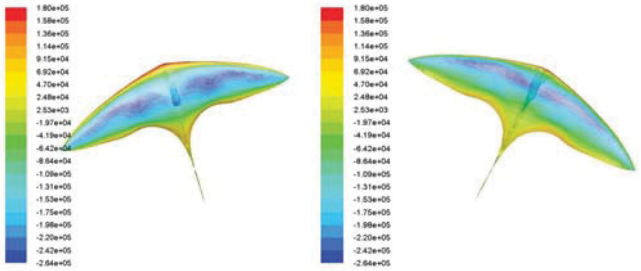

(a)static pressure on direction z (b)static pressure on direction -z

Fig. 4. Static pressure of the manta fish

C. Kinematic Simulation

There are four definitions for dynamic mesh in fluent, which is in the users definition function. The four marcos are DIFINE_CG_MOTION, DEFINE_SDOF_PROPERTIES, DIFINE_GEOM and DEFINE_GRID_MOTION. We use DEFINE_GRID_MOTION as it provides a function of deforming scales. Set the fluctuation frequency of pectoral fin as 2Hz and the fluctuation amplitude as 0.15C. The time step is 0.01s and the motion have to calculate 100 steps to assure the steady state. Carry out simulation I and divide each cycle into ten parts. The results are displayed in fig.5.

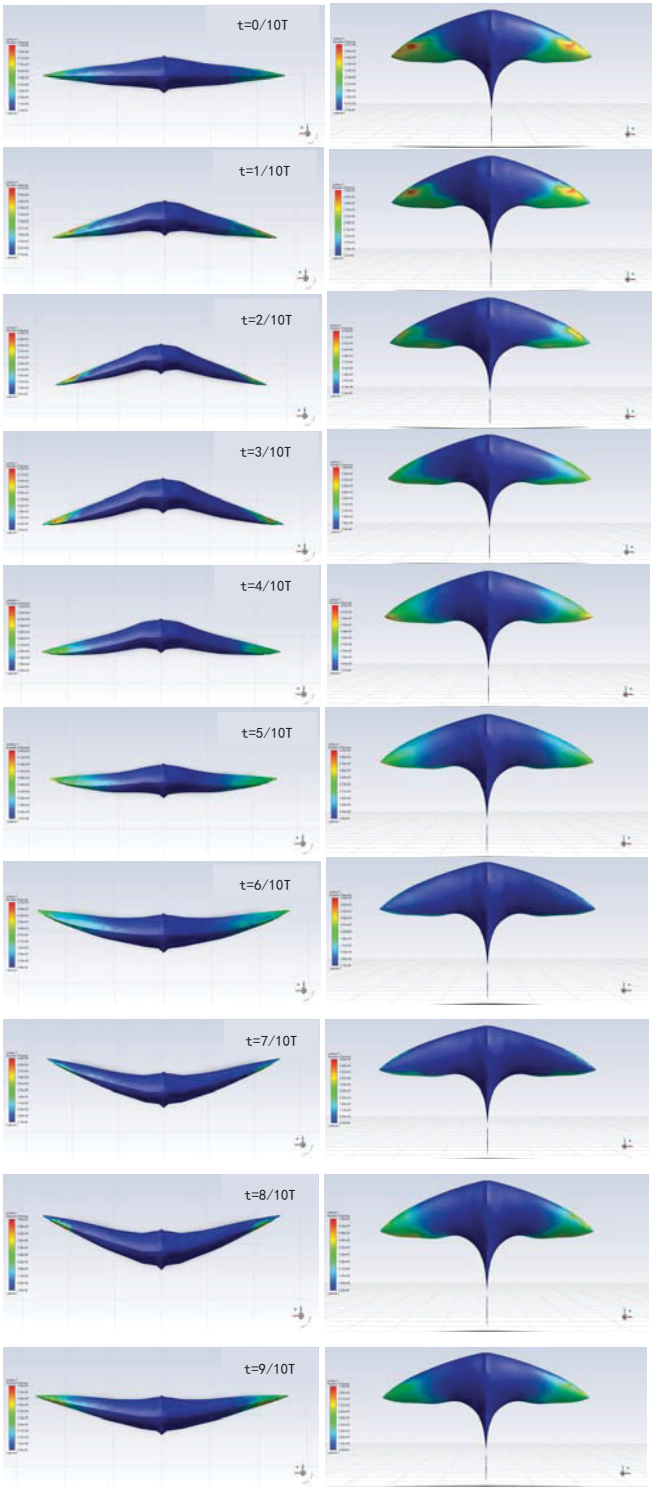

Fig. 5. Dynamic pressure in one cycle when *f=2Hz, A=0.15C*

In order to discuss the relationship between the dynamic pressure change and different fluctuation frequency, we carry out simulation II and set the fluctuation frequency into 4*Hz* and keep the a fluctuation amplitude remains 0.15*C*. The dynamic pressure is shown in fig.6.

In order to discuss the relationship between the dynamic pressure change and different fluctuation amplitude, we carry out simulation III and set the a fluctuation amplitude into 0.075*C* and keep the fluctuation frequency remains *4Hz*. The dynamic pressure is shown in fig.7 and the velocity magnitude is shown in fig.8.

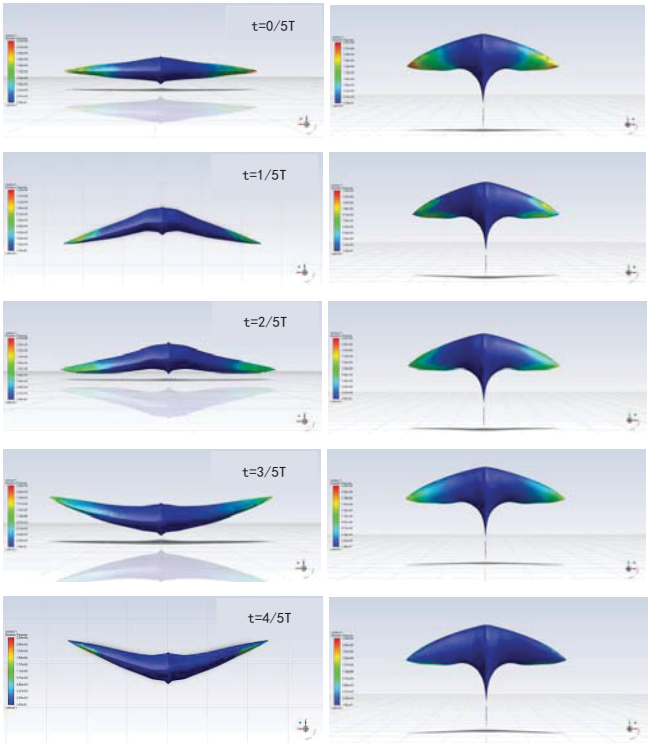

Fig. 6. Dynamic pressure in one cycle when *f=4Hz, A=0.15C*

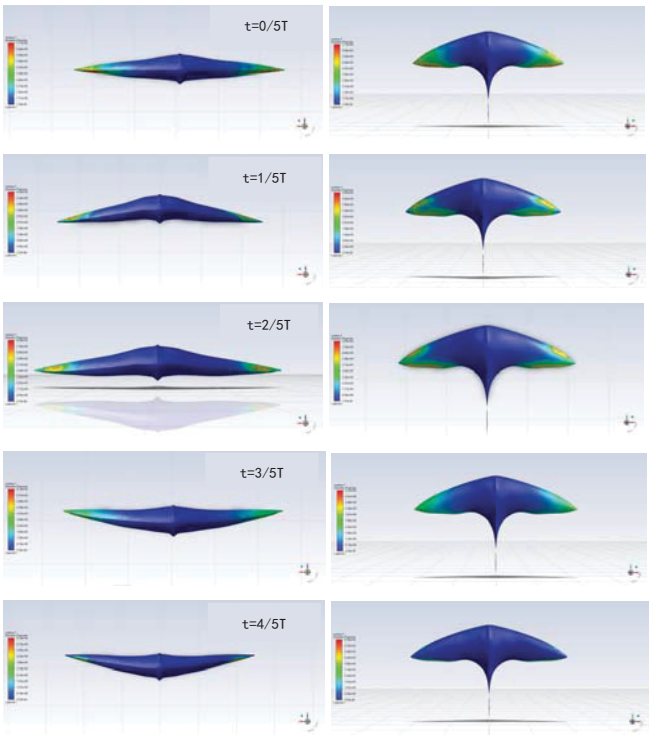

Fig. 7. Dynamic pressure in one cycle when *f=4Hz, A=0.075C*

D. Data Analysis

When the fluctuation amplitude, wave length is constant and increase the fluctuation frequency, the dynamic pressure increases and the drag decrease. And the distribution area of the greater pressure part of the pectoral fin became wider .

When the fluctuation frequency and wave length is constant and increase the fluctuation amplitude, the dynamic pressure increases.

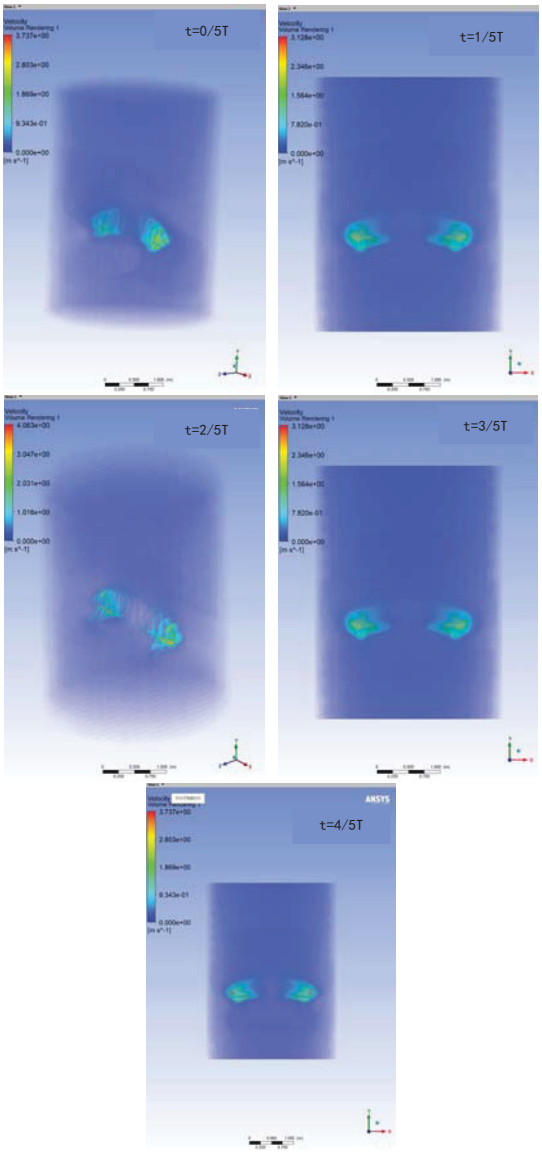

Fig. 8. Velocity magnitude in one cycle when *f=4Hz, A=0.075C*

IV. Conclusion

The simulation shows that during the period of fish motion, the head of the fish is always under positive pressure and the intensity is low. And there is always higher intensity of dynamic pressure on the wing at the end of the wingspan direction. The upwind side of the fin is under positive pressure while the downwind side accepts negative pressure. And this kind of pressure difference arouse the forward swimming process.

The pressure is rooted from the pectoral fins up-flap and down-flap. One movement period include one time up and down. During the up-flap period, a high-pressure center formed from the upwind surface and fall off at the edge of a single petrol fin. During the down-flap period, a high-pressure center also formed and fall off. Therefore, four high-pressure center fall off and provide the pressure difference for manta fish movement, which is consistent with the actual condition.

According to our results, during the period of manta fish motion, the pressure changes of the fish head is very little and has the minium pressure. Therefore, the insensitive part is suited for central control module, which has both enough space and can also reduce the difficulty of waterproof. As for the propel force, we can increase the fluctuation frequency or the fluctuation amplitude to increase the propulsive force. that also convinced that the prototype has a great potential.

Future work will combining dynamics analysis with kinematics equation and make the swimming process more consistence with the actual condition, including swimming in more complex fluid with various postures.

Acknowledgment

This research was supported by National Natural Science Foundation of China (61773064, 61503028), National Key Research and Development Program of China (2017YFB1304404), and National Hightech Research and Development Program (863 Program) of China (No.2015AA043202).

References

[1] W. Wu, C. Liu, F. Li,“ Nanomechanical Properties and Bionic Architecture Design Based on Elytron of Frog-legged Leaf Beetle,” in the 6th International Conference on Bionic Engineering and 2019 International Symposium on nature inspired science and technology, vol:1, 2019.

[2] X.Zhang,“ Elastic local buckling behaviour of beetle elytron plate,” *Journal of Thin-Walled Structures*, vol:165, pp: 107922, 2021.

[3] Z.Wang, B.Li, Q.Luo,“ Effect of wall roughness by the bionic structure of dragonfly wing on microfluid flow and heat transfer characteristics,” *Journal of International Journal of Heat and Mass Transfer*, vol:173, 2021.

[4] W. Bao, L.Gao, H.Wei,“ Effect of 3D printed polycaprolactone scaffold with a bionic structure on the early stage of fat grafting,”*Journal of Materials science & engineering:C*, vol:123, pp: 111973-111973, 2021.

[5] Z. Chen, Y.Li, C.Yao,“ Biomass Shape Memory Elastomers with Rapid Self-Healing Properties and High Recyclability,”*Journal of Biomacromolecules*, vol:6, pp:2768-3776, 2021.

[6] R.Parker,P.Barvara,H.Simon,“ Biomimetic Transparent Eye Protection Inspired by the Carapace of an Ostracod (Crustacea),” *Journal of Nanomaterials*, vol:11, pp:3, 2021.

[7] X. Wang,Z. Li, H.Kang,“ Medical Image Segmentation using PCNN based on Multi-feature Grey Wolf Optimizer Bionic Algorithm,” *Journal of Bionic Engineering*, vol:3, pp:711-720, 2021.

[8] Z.Wang, X.Fang, H.Li,“An improved Partheno-genetic algorithm with reproduction mechanism for the multiple traveling salesperson problem,” *IEEE Access* ,vol:8, pp:102607–102615, 2020.

[9] S. Jagriti, D. Maitreyee, M. Gonçalo,“Fuzzy Inference System Tree with Particle Swarm Optimization and Genetic Algorithm: A novel approach for PM10 forecasting,” *Expert Systems With Applications*, vol:183, pp:115376, 2021.

[10] J. Ji,“Hydrogen peroxide sensor using the biomimetic structure of peroxidase including a metal organic framework,” *Journal* of *Applied Surface Science,* vol:554, pp:121201, 2021.

[11] S. Tvorynska, J. Barek, B. Josypčuk,“Flow amperometric uric acid biosensors based on different enzymatic mini-reactors: A comparative study of uricase immobilization,” *Sensors and Actuators: B. Chemical*, vol:344, pp:130252, 2021.

[12] L.I.E.,A.D.,“ Biology,ecology and conservation of the Mobulidae”, *Journal of fish biology*, vol:80, pp: 1075-1119, APR 2012.

[13] O.Vaughan,“ Robobee breaks free,” *Natural Electronics*, vol:570, pp:491-495, 2019.

[14] T.Wang, Z.Wang, B.Zhang“ Mechanism Design and Experiment of a Bionic Turtle Dredging Robot,” M*achines*, vol:9, 2021, DOI:10.3390.

[15] Y. Wang, S. Sun, M. Xu,“Design of a Bionic Scallop Robot Based on Jet Propulsion,” in *IEEE International Conference on Real-time Computing and Robotics* (RCAR), 2018.

[16] Y.Chen, T.Wang, C.Wu,“Design, control, and experiments of a fluidic soft robotic eel,”*Smart Materials and Structures*, vol:30, 2021, DOI:10.1088.

[17] L.Li, X.Zheng, R. Mao,“Energy Saving of Schooling Robotic Fish in Three-Dimensional Formations,” *IEEE Robotics and Automation Letters*, vol:6, pp:1694-1699, 2021.

[18] Q.Zhao, S. Liu, J. Chen,“Fast-moving piezoelectric micro-robotic fish with double caudal fins,”*Robotics and Autonomous Systems*, vol:140, 2021, DOI: 10.1016.

[19] R. Blake,W., “ Fish Functional Design and Swimming Performance,” *Journal of fish biology*, vol:65, pp:1193-1222, 2004.

[20] L.J.,“Pectoral fin locomotion in batoid fishes: Undulation versus oscillation, ”*Journal of experimental biology*, vol:2, pp:379-394, 2001.

[21] J. Wang, X. Xu, and C. Li, “An improved changing-topology moving mesh method in OpenFOAM ,” in *International Conference on IEEE: Information and Telecommunication Systems(CIT-S)*, 2017 , pp. 239-243, 2017, DOI:10.13140.

[22] H.Davis,A.Rachel,A.Lopes,“On mobulid rays and metals: Metal content for the first Mobula mobular record for the state of Rio de Janeiro, Brazil and a review on metal ecotoxicology assessments for the Manta and Mobula genera,”*Marine pollution bulletin*, vol:168 pp:112472, May, 2021.

[23] Harris, JL,“Fine-scale oceanographic drivers of reef manta ray (Mobula alfredi) visitation patterns at a feeding aggregation site,” vol: 11, pp: 4588-4604, MAY 2021, online.

[24] Palacios, M.D.,“Description of first nursery area for a pygmy devil ray species (Mobula munkiana) in the Gulf of California, Mexico,” *Scentific reports,* vol:11, pp:1, JAN,2021.